

Closed-loop electric currents and non-local resistance measurements with wide F/I/N tunnel contacts

Ya. B. Bazaliy

University of South Carolina, Columbia SC 29208, USA*

R. R. Ramazashvili

Laboratoire de Physique Théorique, Université de Toulouse, CNRS, UPS, France[†]

(Dated: January 28, 2022)

Lateral spin valves are used to generate and characterize pure spin currents. Non-local voltage measured in such structures provides information about spin polarization and spin decay rates. For wide high-transparency F/N contacts it was shown that the Johnson-Silsbee non-local effect is substantially enriched by closed-loop electric currents driven by local spin injection in the electrically dangling part of the valve. For valves with low-transparency F/I/N tunnel contacts such circular currents are strongly suppressed, yet we show that the voltage modifications persist, may be significant, and must be accounted for in the data analysis.

I. INTRODUCTION

A non-local spin valve (NLSV) consists of a normal metal (N) line with two ferromagnetic (F) contacts (Fig. 1). The left contact F_1 injects spin-polarized electrons into N, where they diffuse away from the injection point, producing spin currents j^s both in the left and right directions. At the same time, electric current j cannot enter the electrically dangling part of the circuit on the right—consequently, only spin current is present there.^{1–3} The non-equilibrium electron state driven by such an injection of spin current results in a non-zero voltage V , measured by an ideal voltmeter between the F_2 and N. The absence of j in the electrically dangling part of the valve dictates a very general relation between V and the spin accumulation beneath the contact F_2 , known as the Johnson-Silsbee formula.¹ The voltage V turns out to be independent of the voltmeter probe positions as long as the thickness t_F of the measuring electrode F_2 remains much larger than the spin diffusion length in that material [see Eqs. (6) and (7)].

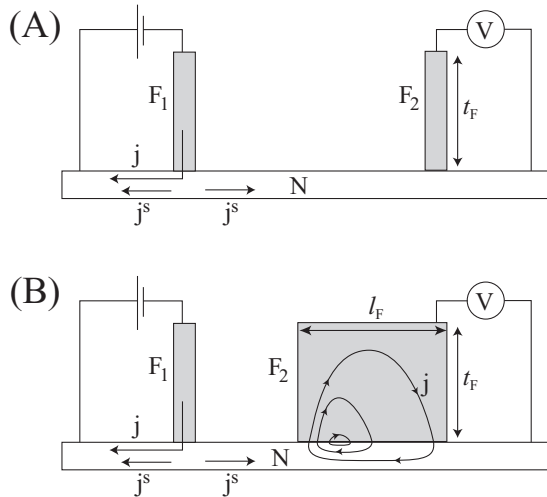


FIG. 1. Non-local spin valve (NLSV) diagram. (A) Narrow measuring contact, no electric current. (B) Wide measuring contact with electric current vortices.

However, it was noticed⁴ that the $j = 0$ condition holds only for narrow F_2 contacts (Fig. 1A). As the width l_F exceeds the scale of appreciable variation of spin accumulation (Fig. 1B), closed-loop electric currents $j \neq 0$ develop, forming a vortex centered at the F_2/N interface. No electric current enters or leaves the electrically dangling (right-hand) part of the device, all current loops are fully contained within it. Crucially, these current loops significantly suppress the measured voltage V and, generally, lead to its dependence on the voltmeter probe positions.

Conclusions of Ref. 4 were reached under the assumption of fully transparent interface between N and F_2 , well satisfied in many realizations of spin valves. At the same time, certain N materials require a tunnel contact for spin injection and detection to overcome the conductivity mismatch problem.^{5,6} As a result, tunnel contact measurements more and more become the method of choice.^{7–18} Will they be affected by the closed-loop electric currents? As shown in Ref. 4, each loop of induced current crosses the F_2/N interface (Fig. 1B) and, in the presence of a tunnel contact, such a current would have to flow across the highly resistive barrier. Naïvely, one would expect a dramatic suppression of such currents by the tunnel barrier, and hence a recovery of the Johnson-Silsbee result.¹ Below we show that such a conclusion is, in fact, incorrect: while the current does decrease with increasing tunnel resistance, nevertheless it significantly suppresses the measured non-local voltage, which may become substantially smaller than the Johnson-Silsbee value.

II. NON-LOCAL VOLTAGE CALCULATION

A. Description of electric and spin transport

We consider electric and spin currents in the diffusive regime, and assume collinear magnetizations of the injector F_1 and detector F_2 electrodes, as is the case in many NLSV measurements. Transport is described by the Valet-Fert equations^{19–22} in the notations of Ref. 4 (see Supplement).

Particle- and spin-current densities j^e, j^s in the bulk are induced by the gradients of electrochemical and spin potentials

μ , μ^s and obey material equations

$$j_i^e = -\frac{\sigma}{e^2} (\nabla_i \mu + \frac{p}{2} \nabla_i \mu^s) \quad (1)$$

$$j_i^s = -\frac{\sigma}{2e^2} (\nabla_i \mu^s + 2p \nabla_i \mu) \quad (2)$$

where $\sigma = \sigma_{\uparrow} + \sigma_{\downarrow}$ is the conductivity of the material and $p = (\sigma_{\uparrow} - \sigma_{\downarrow})/\sigma$ is the “current spin polarization”, present in F only. The spin quantization axis is chosen along the magnetization.

Potential distributions in N and F domains are determined from the electric current conservation and spin current relaxation equations. In the dc regime they read²¹

$$\Delta \mu = -\frac{p}{2} \Delta \mu^s, \quad \lambda_s^2 \Delta \mu^s = \mu^s, \quad (3)$$

with λ_s being the spin diffusion length, denoted as λ_{sN} of λ_{sF} in the corresponding materials.

The tunnel barrier between N and F is necessarily spin-selective, with unequal conductances $\Sigma_{\uparrow} \neq \Sigma_{\downarrow}$.⁶ The current densities through the barrier are

$$j_{\perp}^e = -\frac{\Sigma}{e^2} ([\mu] + \frac{\Pi}{2} [\mu^s]), \quad (4)$$

$$j_{\perp}^s = -\frac{\Sigma}{2e^2} ([\mu^s] + 2\Pi[\mu]), \quad (5)$$

where $\Sigma = \Sigma_{\uparrow} + \Sigma_{\downarrow}$, $\Pi = (\Sigma_{\uparrow} - \Sigma_{\downarrow})/\Sigma$, and $[\mu] = \mu_F - \mu_N$, $[\mu^s] = \mu_F^s - \mu_N^s$ are the potential jumps across the barrier. Eqs. (4) and (5) provide the boundary conditions at the F/N interface.

In terms of spin potential μ^s right beneath the contact F_2 , and the conductivity polarizations p and Π , the Johnson-Silsbee formula states

$$V = p\mu^s/2e, \quad (6)$$

for high-transparency Ohmic contacts, $\Sigma \rightarrow \infty$,¹ and

$$V = \Pi\mu^s/2e \quad (7)$$

for a low-transparency tunnel contacts, $\Sigma \rightarrow 0$.^{6,21}

B. Non-local voltage in the limit of large tunnel resistance

We consider now the right hand side of the NLSV (Fig. 2). Point O is the origin of the (x, y) coordinate system. It is assumed that spin current is uniformly injected along the cross-section OA of the normal line. The tunnel barrier separates N and F along the segment OB of length l_F . The normal wire N is considered to be infinitely long. Accordingly, Eqs. (3) have to be solved in the N and F domains with the following boundary conditions. Along the segment OA , $\mu^s(0)$ is a given constant, and the electric current component normal to OA is zero. At all other outer boundaries, the normal components of both electric and spin currents vanish. At the segment OB Eqs. (4) and (5) relate the vertical current components to potential jumps.

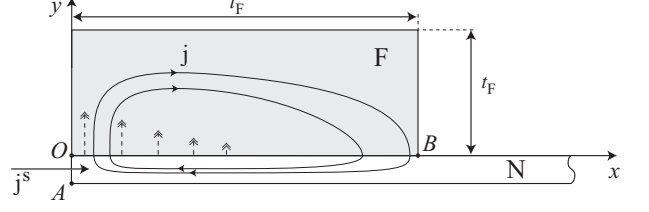


FIG. 2. Right side of NLSV with pure spin current injection. Solid loops show the induced electric currents. Vertical dashed lines with double arrows represent the effective electromotive forces generated at the boundary due to spin accumulation.

For an infinitely high tunnel barrier one has $\Sigma_{\uparrow, \downarrow} = 0$, hence there is no penetration of spins into the F layer. The problem reduces to that of spin diffusion along the N line. With uniform spin injection along OA , the solution reads

$$\mu_0^s(x, y, N) = \mu^s(0) \exp(-x/\lambda_{sN}) \quad (8)$$

in N and $\mu_0^s(x, y, F) = 0$ in F. Furthermore, since the barrier is impenetrable, we essentially deal with two electrically disconnected conductors. Their electrochemical potentials are thus uniform $\mu_0(x, y) = \mu_0(N), \mu_0(F)$ and may assume arbitrary values.

For non-zero but small barrier conductivities given by $\Sigma_{\uparrow, \downarrow} = \varepsilon \tilde{\Sigma}_{\uparrow, \downarrow}$ with $\varepsilon \rightarrow 0$ we seek potentials in the form of Taylor expansion in ε

$$\mu(x, y, D) = \mu_0(D) + \varepsilon \mu_1(x, y, D) + \dots,$$

$$\mu^s(x, y, D) = \delta_{DN} \mu^s(0) e^{-x/\lambda_{sN}} + \varepsilon \mu_1^s(x, y, D) + \dots,$$

where index $D = F, N$ defines the domain and δ_{DN} is the Kronecker symbol.

Finding the current densities in N and F requires calculating $\mu_1(x, y, D)$ and $\mu_1^s(x, y, D)$. However, to first order in ε the non-local voltage can be found without the full solution. From Eq. (4), the leading term of the particle current across the barrier is first order in ε :

$$j_y^e(x, 0) = -\frac{\varepsilon \tilde{\Sigma}}{e^2} \left((\mu_{0F} - \mu_{0N}) + \frac{\Pi}{2} (-\mu_0^s(x, 0, N)) \right) + \dots$$

Particle current conservation requires that the integral $\int_0^{l_F} j_y^e(x, 0) dx$ vanish in the stationary state considered here. To first order in ε this yields

$$(\mu_{0F} - \mu_{0N}) l_F - \frac{\Pi}{2} \int_0^{l_F} \mu_0^s(x, 0, N) dx = 0. \quad (9)$$

Substituting the zeroth-order solution $\mu_0^s(x, 0, N)$ from Eq. (8), we find the measured voltage

$$V = \frac{\mu_{0F} - \mu_{0N}}{e} = \frac{\Pi \lambda_{sN} (1 - e^{-l_F/\lambda_{sN}})}{2e l_F} \mu^s(0).$$

In the limit $l_F \ll \lambda_{sN}$, i.e., when spin accumulation under F is nearly constant, the tunnel Johnson-Silsbee result (7) is recovered. We can now present the voltage drop across the device

of an arbitrary width l_F as

$$V(l_F) = \frac{\lambda_{sN}}{l_F} \left(1 - e^{-l_F/\lambda_{sN}}\right) V_{JS}. \quad (10)$$

Eq. (10) is the central result of our paper. In terms of the “local Johnson-Silsbee voltage” defined as $V_{JS}(x) = \Pi\mu_s(x, 0, N)/(2e)$, Eqs. (9) and (10) can be viewed as averaging $V_{JS}(x)$ over the contact width. However, as the contact width l_F grows, electrochemical potentials in the F and N contacts become significantly non-uniform, and the simple picture above breaks down, as shown in the next section.

C. Validity conditions for the large tunnel resistance approximation

Equations (1) and (4) can be interpreted by taking the point of view that the particle current is produced not only by the electrochemical potential gradients, but also by an additional “effective” electromotive force (EMF) associated with non-uniformity of spin potential.^{6,21,23} Such a view helps one to visualize the emergence of circular currents.⁴ Here we will use it to find the validity range of the approximation of the preceding section, that allowed us to neglect the variations of the electrochemical potentials in the N and F films.

For our device, the effective EMF interpretation leads to an electric circuit analogy, shown in Fig. 3A. Here \mathcal{E}_i represent the effective EMFs, developing across the tunnel barrier due to the jump of μ^s as per Eq. (4). In the $\varepsilon \rightarrow 0$ limit this jump produces the leading, zeroth order contribution to effective EMF, while variation of μ_s in the ferromagnet brings first order corrections in ε . As one moves to the right, away from the spin injection cross-section OA , the jump $[\mu_s] = \mu_s(x, 0, N) + \mathcal{O}(\varepsilon)$ decreases as per Eq. (8), and the corresponding EMFs gradually decay to zero. Resistors R represent the tunneling barrier resistance per unit length. Resistors r represent the distributed resistance of the N and F layers.

Approximation (10) corresponds to neglecting the distributed resistance (r), which yields the circuit shown in Fig. 3B, where the upper and lower horizontal lines are indeed characterized by constant electric potentials V_F and V_N . Applying the Kirchhoff rules to Fig. 3B, one finds the voltage V between F and N:

$$V = V_F - V_N = \frac{\sum_{i=1}^n \mathcal{E}_i}{n}$$

where $i = 1, \dots, n$ labels the EMFs, and n is the total number of vertical legs. This equation is the analogue of the result (10).

Under what conditions can one ignore the resistors r and replace Fig. 3A by Fig. 3B? Obviously, inequality $r \ll R$ has to be satisfied. This, however, is not enough: at the same time, the voltage drop δV along the upper and lower horizontal lines must be much smaller than V .

Horizontal voltage drop δV can be expanded in powers of $r/R \ll 1$, and the leading term, linear in r/R , can be explicitly obtained in terms of the distribution of \mathcal{E}_i (see Appendix). In our problem the \mathcal{E}_i decay with increasing i , reflecting the decay of $\mu_0^s(x, N)$ along the x -axis. The Appendix shows that the

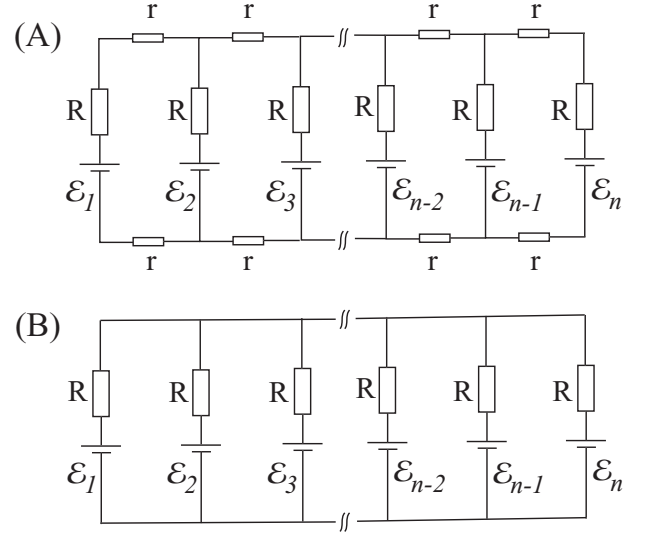


FIG. 3. Electric circuits illustrating the emergence of circular current. Effective EMF's \mathcal{E}_i represent the forces produced by spin potential imbalance. Circuit (A) takes into account the distributed resistance r of the bulk N and F domains. Circuit (B) neglects r as small compared to the resistance R of the tunnel barrier.

ratio $\delta V/V$ increases as the decay becomes more rapid, and only a few first EMFs remain non-zero—that is, as the contact length l_F becomes large compared with the decay length λ_{sN} . This limit constrains r/R the most stringently, as expressed by the inequality

$$r \ll \frac{R}{n^2}.$$

Such a condition shows, in particular, that as the number of vertical legs increases while r/R is kept fixed, the approximation eventually breaks down.

For R representing the tunnel barrier resistance per length Δx , continuous description is recovered by the correspondence

$$R \rightarrow (\Sigma \Delta x)^{-1}, \quad r \rightarrow (\sigma t / \Delta x)^{-1}, \quad n \rightarrow \frac{l_F}{\Delta x}.$$

Here σt stands for either $\sigma_F t_F$ or $\sigma_N t_N$ since we assumed that both N and F lines can be described by the same r . If electric properties of the lines differ by orders of magnitude, a more involved analysis is required.

Together with the inequality $r \ll R/n^2$, this yields the condition

$$\Sigma \ll \frac{\sigma t}{l_F^2}. \quad (11)$$

Inequality (11) can be rewritten as $\Sigma l_F \ll \sigma t / l_F$. Here the left hand side is the total vertical conductance of the tunnel barrier, and the right hand side is the total conductance of the F or N layer in the horizontal direction (more precisely, these are the conductances per unit depth of the device in the direction perpendicular to the plane of Fig. 2).

III. CONCLUSIONS

Expression (10) shows that the non-local voltage measured by a tunneling F/N contact can strongly depend on the contact width. Note that in the limit of low barrier conductance the suppression of voltage is independent of Σ . The latter can be very small, making the circular electric current behind the effect completely negligible. And yet, this current will significantly suppress the non-local voltage.

It is instructive to compare the evolution of non-local voltage in transparent and tunnel barriers contacts. In the former case⁴ there are two regimes: for $l_F \ll \lambda_{sN}$ the voltage is given by $V_{JS} = p\mu_s/2e$ (6), and is independent of voltmeter probe positions; for $l_F \geq \lambda_{sN}$ the voltage becomes probe-position dependent, and decreases compared with (6). In the tunnel contact case there are three regimes: for $l_F \ll \lambda_{sN}$ the voltage is given by $V_{JS} = \Pi\mu_s/2e$ (7), independently of the probe positions; for $\lambda_s \leq l_F \ll \sqrt{\sigma t/\Sigma}$ the voltage is still independent of probe positions but reduces to the value (10); finally, for $l_F \geq \sqrt{\sigma t/\Sigma}$ the voltage becomes probe-position dependent, while being further reduced.

IV. ACKNOWLEDGEMENTS

Ya. B. is grateful to the Laboratoire de Physique Théorique, Toulouse, for the hospitality, and to CNRS for funding the visits. R. R. thanks the Department of Physics & Astronomy for the kind hospitality and support of his visit.

Appendix A: Calculation of the longitudinal voltage

An elementary unit of the original circuit is shown in Fig. 4. Vertical legs are numbered by index $k = 1, 2, \dots, n$. Current through a vertical leg k is related to voltage V_k between points P_k and Q_k as $I_k = (\mathcal{E}_k - V_k)/R$. Due to the symmetry between upper and lower lines, the voltage drop between points P_k and P_{k+1} is $\Delta V_k = (V_k - V_{k+1})/2$. Current through a horizontal leg connecting points P_k and P_{k+1} is then $i_k = \Delta V_k/r$. Current conservation at point P_k gives

$$i_k - i_{k-1} = \frac{\mathcal{E}_k - V_k}{R},$$

or equivalently

$$\Delta V_k = \Delta V_{k-1} + \frac{r}{R}(\mathcal{E}_k - V_k). \quad (\text{A1})$$

It's easy to check that at the left and right ends of the circuit we have to set $\Delta V_0 = 0$ and $\Delta V_n = 0$. This will account for the fact that no current is entering the point P_1 from the left or leaving the point P_n to the right.

First, we express the condition that the sum of currents entering the upper line has to be zero

$$\sum_{k=1}^n I_k = \frac{1}{R} \sum_{k=1}^n (\mathcal{E}_k - V_k) = 0,$$

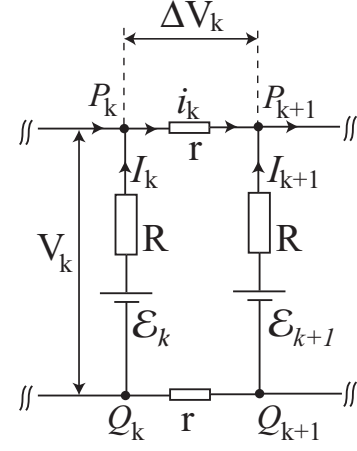


FIG. 4. A unit of the effective circuit.

or

$$\sum_{k=1}^n V_k = \sum_{k=1}^n \mathcal{E}_k.$$

The average vertical voltage between the upper and lower lines, $\bar{V} = (\sum V_k)/n$ is then

$$\bar{V} = \frac{\sum_{k=1}^n \mathcal{E}_k}{n}. \quad (\text{A2})$$

Next, we wish to express the horizontal voltage drop δV between the points P_1 and P_n , so that we can later require $\delta V \ll \bar{V}$ to make the average voltage a meaningful quantity. Using (A1) and $\Delta V_0 = 0$ we can write

$$\begin{aligned} \Delta V_1 &= \frac{r}{R}(\mathcal{E}_1 - V_1), \\ \Delta V_2 &= \Delta V_1 + \frac{r}{R}(\mathcal{E}_2 - V_2) = \frac{r}{R}((\mathcal{E}_1 - V_1) + (\mathcal{E}_2 - V_2)), \\ &\dots \\ \Delta V_k &= \frac{r}{R}((\mathcal{E}_1 - V_1) + (\mathcal{E}_2 - V_2) + \dots + (\mathcal{E}_k - V_k)). \end{aligned}$$

The total horizontal voltage drop between P_1 and P_n can be then expressed by summing these voltage drops

$$\begin{aligned} \delta V &= \sum_{k=1}^{n-1} \Delta V_k = \frac{r}{R}[(n-1)(\mathcal{E}_1 - V_1) + (n-2)(\mathcal{E}_2 - V_2) + \dots \\ &\quad + (n-k)(\mathcal{E}_k - V_k) + \dots + (\mathcal{E}_{n-1} - V_{n-1})]. \end{aligned}$$

Clearly, for $r = 0$ one gets $\delta V = 0$ and $V_k = \bar{V}$ for all k 's. For non-zero r we can consider an expansion in powers of $r/R \ll 1$

$$V_k = \bar{V} + \left(\frac{r}{R}\right) V_{k1} + \left(\frac{r}{R}\right)^2 V_{k2} + \dots$$

Then in the first order in r/R the total horizontal voltage drop is

$$\delta V \approx \frac{r}{R} \sum_{k=1}^{n-1} (n-k)(\mathcal{E}_k - \bar{V}). \quad (\text{A3})$$

This is an explicit formula for δV in terms of the given set of \mathcal{E}_k 's. Note that it excludes the leftmost EMF \mathcal{E}_n , however, using the identity $\sum_{k=1}^n (\mathcal{E}_k - \bar{V}) = 0$ that follows from (A2), and adding it to (A3), one can rewrite it so that all EMF's are present on equal footing

$$\delta V \approx \frac{r}{R} \sum_{k=1}^n (n+1-k)(\mathcal{E}_k - \bar{V}). \quad (\text{A4})$$

Total horizontal voltage drop δV depends on the distribution of EMF's. For example, in the absence of spatial variation, $\mathcal{E}_k = \text{const}$, Eq. (A4) gives $\delta V = 0$, regardless of the value of r .

The more spatial variation of EMF's there is, the larger be-

comes δV . This can be illustrated by an example, where the first $p < n$ EMFs are equal and non-zero, $\mathcal{E}_1 = \mathcal{E}_2 = \dots = \mathcal{E}_p = \mathcal{E}$, while all the following EMFs vanish: $\mathcal{E}_{p+1} = \mathcal{E}_{p+2} = \dots = \mathcal{E}_n = 0$. For such an EMF distribution the average voltage is $\bar{V} = (p/n)\mathcal{E}$, and Eq. (A4) leads—after some algebra—to

$$\delta V = \frac{r}{R} \frac{n(n-p)}{2} \bar{V}.$$

Whenever p is small enough compared with n , so that $(n-p) \sim n$, this formula yields $\delta V \sim \bar{V} n^2 r / R$, and condition $\delta V \ll \bar{V}$ then leads to a requirement

$$r \ll \frac{R}{n^2}. \quad (\text{A5})$$

-
- * yar@physics.sc.edu
† revaz@irsamc.ups-tlse.fr
- ¹ M. Johnson and R. H. Silsbee, *Interfacial charge-spin coupling: Injection and detection of spin magnetization in metals*, Phys. Rev. Lett. **55**, 1790 (1985).
 - ² M. Johnson and R. H. Silsbee, *Thermodynamic analysis of interfacial transport and of the thermomagnetolectric system*, Phys. Rev. B **35**, 4959 (1987).
 - ³ M. Johnson and R. H. Silsbee, *Calculation of nonlocal base-line resistance in a quasi one-dimensional wire*, Phys. Rev. B **76**, 153107 (2007).
 - ⁴ Ya. B. Bazaliy and R. R. Ramazashvili, *Local injection of pure spin current generates electric current vortices*, Appl. Phys. Lett. **110**, 092405 (2017); doi: 10.1063/1.4977027
 - ⁵ G. Schmidt, D. Ferrand, L. W. Mollenkamp, A. T. Filip, and B. J. van Wees, *Fundamental obstacle for electrical spin injection from a ferromagnetic metal into a diffusive semiconductor*, Phys. Rev. B **62**, R4790 (2000).
 - ⁶ E. I. Rashba, *Theory of electrical spin injection: Tunnel contacts as a solution of the conductivity mismatch problem*, Phys. Rev. B **62**, R16267 (2000).
 - ⁷ B. T. Jonker, G. Kioseoglou, A. T. Hanbicki, C. H. Li, and P. E. Thompson, *Electrical spin-injection into silicon from a ferromagnetic metal/tunnel barrier contact*, Nature Phys. **3**, 542 (2007).
 - ⁸ S. P. Dash, S. Sharma, R. S. Patel, M. P. de Jong, and R. Jansen, *Electrical creation of spin polarization in silicon at room temperature*, Nature **462**, 26 (2009).
 - ⁹ M. Tran, H. Jaffrés, C. Deranlot, J.-M. George, A. Fert, A. Miard, and A. Lemaître, *Enhancement of the Spin Accumulation at the Interface between a Spin-Polarized Tunnel Junction and a Semiconductor*, Phys. Rev. Lett. **102**, 036601 (2009).
 - ¹⁰ C.H. Li, O.M.J. van t Erve, and B.T. Jonker, *Electrical injection and detection of spin accumulation in silicon at 500 K with magnetic metal/silicon dioxide contacts*, Nature Comm. **2**, 245 (2011).
 - ¹¹ W. Han, X. Jiang, A. Kajdos, S.-H. Yang, S. Stemmer, and S. S. P. Parkin, *Spin injection and detection in lanthanum- and niobium-doped SrTiO₃ using the Hanle technique*, Nature Comm. **4**, 2134 (2013).
 - ¹² O.M.J. van t Erve, A.L. Friedman, C.H. Li, J.T. Robinson, J. Connell, L.J. Lauhon, and B.T. Jonker, *Spin transport and Hanle effect in silicon nanowires using graphene tunnel barriers*, Nature Comm. **6**, 7541 (2015).
 - ¹³ M. Drögeler, C. Franzen, F. Volmer, T. Pohlmann, L. Banzerus, M. Wolter, K. Watanabe, T. Taniguchi, C. Stampfer, and B. Beschoten, *Spin Lifetimes Exceeding 12 ns in Graphene Nonlocal Spin Valve Devices* Nano Lett. **16**, 3533 (2016).
 - ¹⁴ M. Gurram, S. Omar, and B. J. van Wees, *Bias induced up to 100% spin-injection and detection polarizations in ferromagnet/bilayerhBN/graphene/hBN heterostructures*, Nature Comm. **8**, 248 (2017).
 - ¹⁵ A. Dankert and S. P. Dash, *Electrical gate control of spin current in van der Waals heterostructures at room temperature*, Nature Comm. **8**, 16093 (2017).
 - ¹⁶ A. Avsar, J. Y. Tan, M. Kurpas, M. Gmitra, K. Watanabe, T. Taniguchi, J. Fabian and B. Özyilmaz, *Gate-tunable black phosphorus spin valve with nanosecond spin lifetimes*, Nature Physics **13**, 888 (2017).
 - ¹⁷ J. C. Leutenantsmeyer, J. Ingla-Aynés, J. Fabian, and B. J. van Wees, *Observation of Spin-Valley-Coupling-Induced Large Spin-Lifetime Anisotropy in Bilayer Graphene*, Phys. Rev. Lett. **121**, 127702 (2018).
 - ¹⁸ A. Spiesser, Y. Fujita, H. Saito, S. Yamada, K. Hamaya, S. Yuasa, and R. Jansen, *Hanle spin precession in a two-terminal lateral spin valve*, Appl. Phys. Lett. **114**, 242401 (2019).
 - ¹⁹ I. A. Campbell, A. Fert, and A. R. Pomeroy, *Evidence for Two Current Conduction in Iron*, Phil. Magazine **15**, 977, (1967).
 - ²⁰ T. Valet and A. Fert, *Theory of the perpendicular magnetoresistance in magnetic multilayers*, Phys. Rev. B **48**, 7099 (1993).
 - ²¹ E. I. Rashba, *Diffusion theory of spin injection through resistive contacts*, Eur. Phys. J. B **29** 513 (2002).
 - ²² S. Takahashi and S. Maekawa, *Spin injection and detection in magnetic nanostructures*, Phys. Rev. B **67**, 052409 (2003).
 - ²³ J. Fabian, A. Matos-Abiague, C. Ertler, P. Stano, and I. Zutic, *Semiconductor spintronics*, Sec. II-D, Acta Physica Slovaca **57**, 565 (2007).

Supplement

to Ya. B. Bazaliy and R. R. Ramazashvili,
 “Closed-loop electric currents and non-local resistance measurements with
 wide F/I/N tunnel contacts”.

Notation for spin and charge diffusion equations

In the Valet-Fert model carrier distributions for spin $\alpha = \uparrow, \downarrow$ are characterized by different electrochemical potentials μ_α . Currents \mathbf{j}_σ (vectors in real space) are defined here as particle number currents. To obtain electric currents, they should be multiplied by electron charge. With two conductivities $\sigma_{\uparrow, \downarrow}$ being different in a ferromagnet, the currents carried by the two spin populations are given by $\mathbf{j}_\alpha = -(\sigma_\alpha/e^2)\nabla\mu_\alpha$.

Electric current $\mathbf{j} = \mathbf{j}_\uparrow + \mathbf{j}_\downarrow$ is conserved and the total electron density $n = n_\uparrow + n_\downarrow$ obeys

$$\partial_t n + \text{div} \mathbf{j} = 0 .$$

The spin current $\mathbf{j}^s = \mathbf{j}_\uparrow - \mathbf{j}_\downarrow$ is not conserved due to the spontaneous relaxation of spin.

In the normal metal $\sigma_\uparrow = \sigma_\downarrow$, and in equilibrium $n_\uparrow = n_\downarrow$. For small nonequilibrium spin density $n_s = n_\uparrow - n_\downarrow$, spin decay is characterized by a relaxation time τ_s , so that spin current and spin density are related by

$$\partial_t n^s + \text{div} \mathbf{j}^s = -\frac{n_s}{\tau_s} .$$

In a steady state one finds

$$\text{div} \mathbf{j} = 0, \quad \text{div} \mathbf{j}^s = -n_s/\tau_s .$$

Particle and spin currents in a normal metal can be expressed through the average potential $\mu = (\mu_\uparrow + \mu_\downarrow)/2$ (the quantity measured by an ideal voltmeter), and the spin potential $\mu^s = \mu_\uparrow - \mu_\downarrow$ that characterizes the non-equilibrium spin accumulation. With $\sigma = \sigma_\uparrow + \sigma_\downarrow$ one finds

$$\mathbf{j} = -\frac{\sigma}{e^2} \nabla \mu , \quad \mathbf{j}^s = -\frac{\sigma}{2e^2} \nabla \mu^s .$$

Spin accumulation and spin potential are related by the density of states ν as $n_s = \nu\mu^s$, giving

$$\text{div}\mathbf{j} = 0, \quad \text{div}\mathbf{j}^s = -\nu\mu^s/\tau_s. \quad (1)$$

or, assuming spatially uniform material parameters,

$$\Delta\mu = 0, \quad \Delta\mu^s = \frac{\mu^s}{\lambda_s^2} \quad (2)$$

with spin diffusion length $\lambda_s = \sqrt{\sigma\tau_s/(2\nu e^2)}$.

In a ferromagnet $\sigma_\uparrow \neq \sigma_\downarrow$, and the currents \mathbf{j} and \mathbf{j}^s can be written as

$$\mathbf{j} = -\frac{\sigma}{e^2}(\nabla\mu + \frac{p}{2}\nabla\mu^s) \quad (3)$$

$$\mathbf{j}^s = -\frac{\sigma}{2e^2}(\nabla\mu^s + 2p\nabla\mu) \quad (4)$$

with polarization $p = (\sigma_\uparrow - \sigma_\downarrow)/\sigma$. Note that in the Eqs. (3-4) spin and charge are coupled by $p \neq 0$. Spin relaxation description in a ferromagnet is more complicated and involves two spin-dependent densities of states $\nu_\uparrow, \nu_\downarrow$.¹ The steady state equations acquire the form

$$\Delta\mu = -\frac{p}{2}\Delta\mu^s, \quad \lambda_s^2\Delta\mu^s = \mu^s, \quad (5)$$

with λ_s being the appropriately defined¹ spin relaxation length in a ferromagnet. Note that the second equation on μ_s does not involve the electric potential μ for either normal metal or ferromagnet. However, the two are coupled for $p \neq 0$ by the first equation.

¹E. I. Rashba, Eur. Phys. J. B **29**, 513 (2002) *Diffusion theory of spin injection through resistive contacts*.